Strengthening and Toughening of Thermoplastic Polyolefin Elastomer Using Polypropylene-Grafted Multiwalled Carbon Nanotubes

Chaoqun Li, Hua Deng, Ke Wang, Qin Zhang, Feng Chen, Qiang Fu

College of Polymer Science and Engineering, State Key Laboratory of Polymer Materials Engineering, Sichuan University, Chengdu 610065, China

Received 9 July 2010; accepted 30 November 2010
DOI 10.1002/app.33892
Published online 14 March 2011 in Wiley Online Library (wileyonlinelibrary.com).

ABSTRACT: In this article, it is demonstrated that simultaneously strengthened and toughened nanocomposites based on polypropylene/EPDM thermoplastic elastomer (TPO) matrix can be achieved through enhanced adhesion between MWNTs and polymer matrix by using PP grafted multiwalled carbon nanotubes (MWNTs). To improve the interface between filler and matrix, MWNTs were treated with acid, or covalently linked to polypropylene. The chemical and morphological transformation of the modified MWNTs, and its effect on the morphology and mechanical properties of the composites are investigated. The strengthening and toughening mechanism is discussed regarding the structural property relationship. © 2011 Wiley Periodicals, Inc. J Appl Polym Sci 121: 2104–2112, 2011

Key words: thermoplastic polyolefin; carbon nanotubes; strengthening and toughening

INTRODUCTION

Carbon nanotubes (CNTs) possess excellent electronic, mechanical and thermal properties due to their unique structure; it shows much potential in reinforcing polymer matrix. However, CNTs tend to aggregate and entangle together due to their small size, high surface energy and intrinsic van der Waals force.[1–3] Therefore, achieving homogeneous dispersion of CNTs in polymer matrix and good adhesion between filler and matrix is the one of the keys to prepare high performance polymer/CNT nanocomposites.[4–6] Many researches have been carried out to improve the dispersion of CNTs in polymers as well as the adhesion between CNTs and polymer matrix. Methods including chemical modification, polymer chain wrapping, ultrasonication, aid of surfactants etc. have been adopted.[5,7–17] Because of the large surface area and polar nature of carbon nanotubes, it is extremely hard to disperse them uniformly in nonpolar polyolefin matrices. Compatibilizers such as maleic anhydride grafted polymer were often introduced to stabilize the morphology as well as improve the interfacial adhesion between CNTs and polymer matrix. It is probably the functional groups of compatibilizer would wet CNTs through hydrogen bond formation, ionic-polar interaction or covalent linkage.[18–21] Goh et al.[18,19] used polyolefin grafted maleic anhydride to react with amine-functionalized MWNTs and successfully grafted polyolefin molecular chains onto MWNTs. Upon the incorporation of polyolefin grafted MWNTs, a significant improvement in mechanical properties were obtained. Besides, the state of dispersion of MWNTs and the phase adhesion can be improved even by nonconvalent treatments. It was reported polymers containing aromatic groups were easy on wetting MWNTs. For example, noncovalent surface modication of nanotubes through interaction between MWNTs and phenyl groups can be built during blending MWNTs with polystyrene.[22,23]

Numerous investigations have been carried out on strengthening polymer matrix with carbon nanotubes. However, only few studies concentrate on polymer blends based on thermoplastic elastomer (TPO), despite of the fact that it has many commercial applications, particularly in automotive interiors, where TPOs based on uncured ethylene–propylene–diene teropolyemr (or ethylene octene copolymer) and polypropylene is often used. Inorganic fillers are commonly added into TPO formulations to enhance their stiffness. The use of fillers such as nano-silica and clay for the modification of TPOs has been studied in recent years.[24–28] However, there are few studies concerning carbon nanotubes modified TPOs[29,30]

Correspondence to: H. Deng (huadeng@scu.edu.cn) and Q. Fu (qiangfu@scu.edu.cn).

Contract grant sponsor: Special Funds for Major State Basic Research Projects of China; contract grant number: 973 program, 2011CB606006.

Contract grant sponsor: National Natural Science Foundation of China; contract grant number: 51003063.

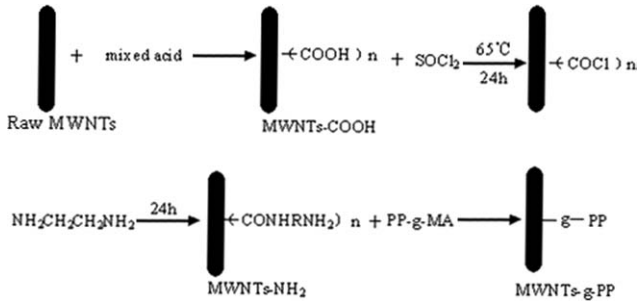

Figure 1 The procedures used for the functionalization of MWNTs.

and even fewer report focus on strengthening TPOs with carbon nanotubes. In present work, TPO/ MWNTs nanocomposites were prepared by simple melt compounding. MWNTs were modified with acid, surfactant or grafted onto polymer chains, respectively, to control the adhesion between nanofiller and polymer matrix. The structural-property relationship of the composites was discussed.

EXPERIMENTAL

Materials

Commercially available isotactic polypropylene (Ning Xia Petroleum, China) with a melt flow index (MFI) of 2.5 g/min (190°C, 2.16 kg) was used. EPDM (4770R, ethyldiene norborene (ENB) type) was supplied by DuPont Co. (United States) with an ethylene content of 70% and a ML_{1+4} value of 70 at 100°C. The compatibilizer, PP grafted maleic anhydride (PP-*g*-MA) (MA content0.9 wt %, MFI6.74 g/min at 190°C) in which maleic anhydride group is randomly grafted on a PP backbone, was purchased from Chen Guan Co. (Sichuan, China). MWNTs (purity > 95%, diameter within 106537420 nm) was purchased by Shenzhen Nanotech Port Co. Ltd., China.

Modification of MWNTs

The preparation of MWNTs-COOH

Three grams of MWNTs were treated with 300 mL mixed solution of concentrated sulfuric acid and nitric acid (3 : 1 by volume, respectively) at 45°C for 5 h. After that, MWNTs-COOH were filtrated and washed by distilled water and repeat filtration until the pH reaches 7. Then, MWNTs-COOH was dried at 80°C in vacuum oven for 24 h.

The preparation of MWNTs-g-PP

MWNTs-COOH (1 g) was stirred in thionyl chloride ($SOCl_2$) at 65°C for 24 h. After acyl chlorination, the MWNTs were centrifuged and washed with anhydrous tetrahydrofuran (THF) for five times, and dried under vacuum at 40°C for 30 min. Then, the dried acyl-chlorinated MWNTs was reacted with ethylenediamine at room temperature for 24h. The final product was washed with THF, and then they were dried at 40°C in vacuum oven to obtain MWNTs-NH_2.

PP-*g*-MA and MWNTs-NH_2 were blended via a simple melt compounding method using a Haake Mini-Lab twin-screw extruder (Thermo Electron Corp.) under the condition of 100 rpm and 220°C. The weight ratio between PP-*g*-MA and MWNTs-NH_2 was kept at 4 : 1 to ensure a complete conversion of amine groups in MWNTs-NH2 to imide groups. The final product prepared is PP grafted MWNTs (MWNTs-*g*-PP). This method is similar to the method Goh et al. has reported.[18,19] The schematic of the whole reaction procedure is shown in Figure 1.

Fabrication of TPO/MWNTs nanocomposites

The preparation of TPO/MWNTs nanocomposites composed of various amount of MWNTs was performed in a Brabender mixer at temperature of 190°C and rotor speed of 80 rpm. The compounding was carried out by firstly blending the PP powder, PP-*g*-MA with raw MWNTs or modified MWNTs for 10 min, and then EPDM was added and blended for another 10 min. In addition, neat TPO was prepared under the same condition for comparison. The composition of the prepared samples is listed in Table I.

TABLE I
Formulations of the Prepared Samples

Samples name	PP/ EPDM (wt %)	PP-MA (wt %)	MWNTs (wt %)	MWNTs-COOH (wt %)	MWNTs-g-PP (wt %)
Pure TPO	88	12			
TPO/ MWNTs	85	12	3		
TPO/ MWNTs -COOH	85	12		3	
TPO/ MWNTs-g-PP	85				15

Please note that the weight ratio of PP/ EPDM is 20 : 80 wt % for all samples, and the MWNTs content in MWNTs-g-PP is 20 wt %.

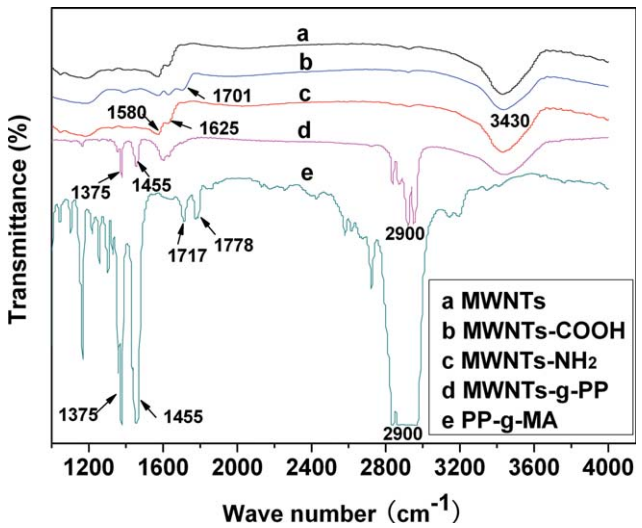

Figure 2 FTIR spectras of (a) raw MWNTs, (b) MWNTs-COOH, (c) MWNTs-NH_2. [Color figure can be viewed in the online issue, which is available at wileyonlinelibrary.com.]

Characterization

Fourier transform infrared (FTIR) spectra were measured on a Nicolet IS10 spectrophotometer in transmission mode. Samples were mixed with KBr, and the resulting mixture was pressed into disks for FTIR test. A background spectrum containing no sample was subtracted from the spectra.

Thermogravimetric analysis (TGA, WRT-2P) was carried out at a heating rate of 10°C/min from room temperature to 700°C in nitrogen atmosphere. For FTIR and TGA test, the functionlized MWNTs in the mixture were dissolved in xylene, the solution were filtered, this procedure was repeated five times to remove unreacted PP-*g*-MA. Then, it is washed with THF for four to five cycles to ensure complete removal of un-reacted PP-*g*-MA.

SEM experiment was carried out to examine the morphology of CNTs and TPO/CNT nanocomposites. The composites samples were fractured in liquid nitrogen or etched with xylene at room temperature. Then the fractured surfaces or etched surfaces were gold-coated and investigated with SEM (Inspect F, FEI company) with an acceleration voltage of 20 kV. The SEM of CNTs was conducted on as-prepared CNTs samples.

Tensile experiments were carried out with aid of Shimadzu AG-10TA Universal Testing Machine. The crosshead speed of crosshead was 100 mm/min. The values were calculated as averages over five specimens for each composition.

Dynamic mechanical analysis of samples was carried out using a dynamic mechanical analyzer (Q800, TA Company) in tension mode with following parameters: frequency 1 Hz; strain amplitude 40 μm; scan rate 3°C/min, in the temperature range of −100 to 100°C.

RESULTS AND DISCUSSION

FTIR analysis of MWNTs

The FT-IR spectrum of the Raw MWNTs and surface treated MWNTs are shown in Figure 2. The acid treated MWNTs show new peaks in comparison with the FT-IR spectrum of untreated MWNTs, the peaks at 1701 cm^{-1} is assigned to the C=O stretching vibration, demonstrating the introduction of carbonyl groups on the surface of MWNTs,[31] the broad peak present at 3430 cm^{-1} is the stretching vibration of —OH functional group which is already reported by our previous report and some other works.[32,33] For amino functionalized MWNTs (curve c), the peak of C=O stretching vibration shift from 1701 cm^{-1} to 1625 cm^{-1}, the peak at 1580 cm^{-1} is the bending vibration of $-NH_2$ functional group. While for PP-*g*-MA, the peak at 1375 cm^{-1} and 1455 cm^{-1} are assigned to bending vibration of CH_3, the peak at 1717 cm^{-1} and 1778 cm^{-1} is attributed to C=O stretching vibration of maleic anhydride, the peak at around 2900 cm^{-1} represents the stretching vibration of C—H.[34] Comparing curve d with e, the peak at 1375 cm^{-1}, 1455 cm^{-1}, and 2900 cm^{-1} remains in MWNTs-*g*-PP, indicates that MWNTs-NH_2 have been grafted onto PP-*g*-MA during melt mixing.[35]

Raman analysis of MWNTs

Figure 3 shows the Raman spectra of MWNTs, MWNTs-COOH and MWNTs-*g*-PP. There are two significant peaks in Raman spectra which are considered to be the characteristic peaks of MWNTs, namely the D band at about 1350 cm^{-1} and the G band at 1580 cm^{-1}. The D- to G-band intensity ratio (I_D/I_G) is typically taken as a measure standard of

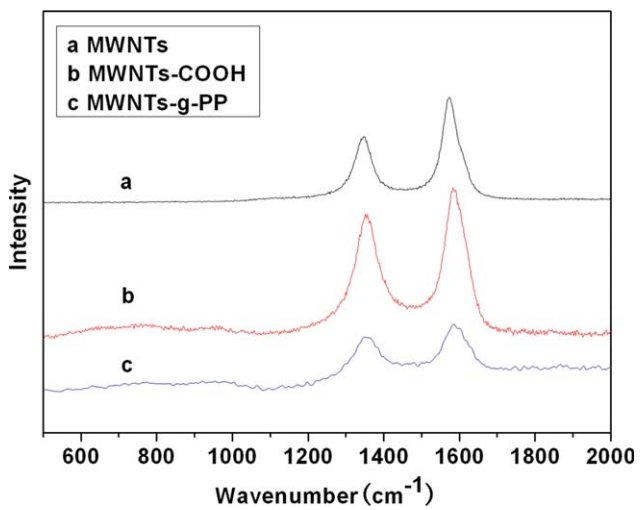

Figure 3 The raman spectra of raw MWNTs(a), MWNTs-COOH(b), and MWNTs-*g*-PP(c). [Color figure can be viewed in the online issue, which is available at wileyonlinelibrary.com.]

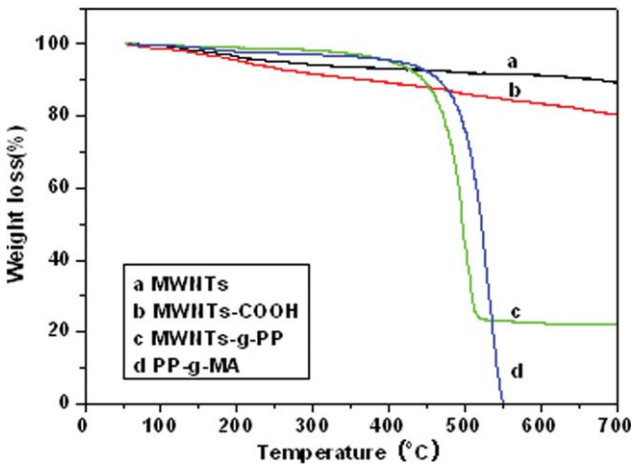

Figure 4 TGA analysis of (a) raw MWNTs, (b) MWNTs-COOH, (c) MWNTs-*g*-PP, (d) PP-*g*-MA. [Color figure can be viewed in the online issue, which is available at wileyonlinelibrary.com.]

surface defects in CNTs.[36] For MWNTs the intensity ratio(I_D/I_G) is 0.56. It is clearly observed that the increment in the defects in the nanotube lattice after the strong acid treatment. The I_D/I_G intensity ratio increased to 0.78. However, the defects in MWNTs may assist the chemical grafting of polymers to the surface of MWNTs. The Raman spectroscopy results of MWNTs-COOH are consistent with those found in other researches.[21,37] While the I_D/I_G ratio of MWNTs-g-PP is close to that of MWNTs-COOH, indicating the function procedure has not further damaged the structure of MWNTs.[38]

TGA characterization

Figure 4 shows the TGA curves of raw MWNTs, MWNTs-COOH, PP-*g*-MA, and MWNTs-*g*-PP. TGA spectrum of raw MWNTs shows 8% weight lost below 600°C. The weight lost for MWNTs-COOH is more than 16%, indicating that -COOH has been grafted onto MWNTs. The TGA spectrum of MWNTs-*g*-PP exhibits a large weight loss which can be attributed to the thermal degradation of attached polypropylene polymer chains. The remaining solid for MWNTs-*g*-PP above 600°C is about 22 wt %. It might be due to the fact that MWNTs-*g*-PP contains nearly 80 wt % of PP-*g*-MA, as the ratio between PP-*g*-MA and MWNTs is 4 : 1. Therefore, TGA result proves that most of PP-*g*-MA have successfully grafted onto MWNTs.

Morphology of MWNTs

Figure 5 shows the morphology of raw MWNTs, MWNTs-COOH and MWNTs-*g*-PP. The raw MWNTs shown in Figure 5(a) are randomly folded

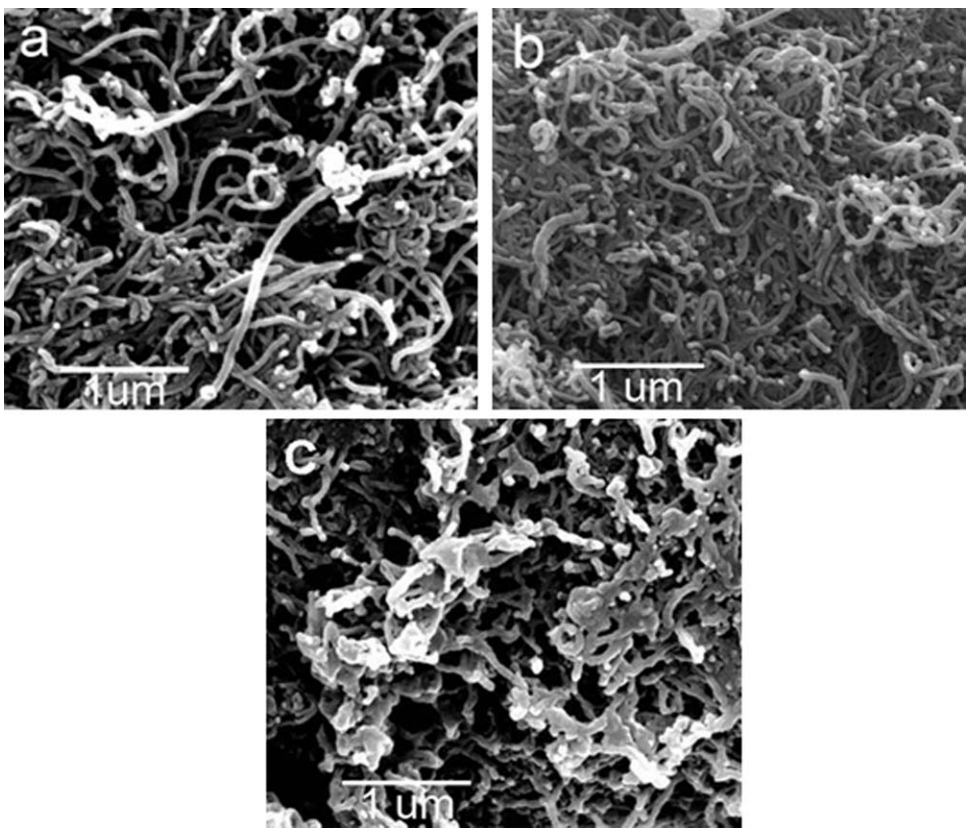

Figure 5 SEM micrographs of (a) Raw MWNTs, (b) MWNTs-COOH, and (c) MWNTs-*g*-PP.

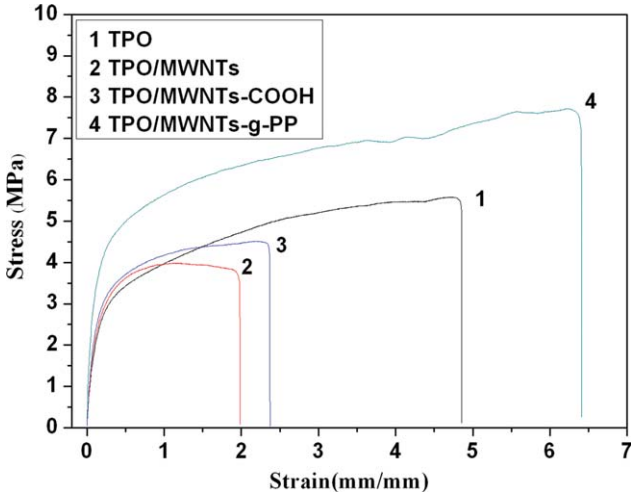

Figure 6 Stress–strain behavior of pure TPO (Curve 1), TPO/MWNTs (Curve 2), TPO/MWNTs-COOH (Curve 3), TPO/MWNTs-*g*-PP (Curve 4). [Color figure can be viewed in the online issue, which is available at wileyonlinelibrary.com.]

and loosely entangled. The length of MWNTs-COOH was greatly reduced due to the strong oxidation during mixed acid treatment.[3] Moreover, MWNTs-COOH shows a more compact stacking morphology comparing with raw MWNTs, as acid modification have introduced large amount of hydroxyl and carboxyl groups on the sidewall of MWNTs (see Fig. 2) and strengthened the van der Waals attraction between them. Similar study has been reported in literature.[39,40] As a result, it may be more difficult to disperse MWNTs in polymer matrix and the mechanical properties of the composites might be damaged.

By contrast, MWNTs-*g*-PP [Fig. 5(c,d)] were wrapped by polymer chains and displayed a cotton-like structure, the diameter of MWNTs-*g*-PP is larger than that of raw MWNTs and MWNTs-COOH. Both randomly folded and compact stacked structures of MWNTs-*g*-PP can be found, some bundles of MWNTs-*g*-PP were crosslinked together by the functional groups. Besides, blurring of the images of MWNTs-*g*-PP are observed, it might be caused by the decreased electrical conductivity due to chemical modification of MWNTs surface.[37,41] In summary, the wrapping and interconnection bonding of MWNTs-*g*-PP has been successfully created and it would improve the dispersion of carbon nanotubes in polymer matrix, and enhance load transfer between filler and matrix.

Tensile properties

Typical stress–strain curves for pure TPO and TPO/MWNTs nanocomposites are shown in Figure 6. It can be observed that the tensile properties of the composites are significant different comparing with pure TPO as summarized in Table II. The elastic modulus of TPO/MWNTs-*g*-PP is nearly 150% higher than that of pure TPO, the tensile strength is improved by about 30%, the elongation at break also shows moderate increases, indicating that an increase in toughness has been obtained for the composites. According to the increase in the area under stress–strain curve,[5,18] a 67% increase in toughness has been obtained for TPO/MWNTs-*g*-PP composites. This significant enhancement in the mechanical properties suggests an excellent dispersion of MWNTs-*g*-PP in TPO matrix. As interaction between TPO matrix and MWNTs is relatively weak due to the nonpolar nature of TPO matrix, the functionalization of MWNTs with PP chains could enhance the interaction between the filler and matrix. Such an enhancement in mechanical properties has confirmed that the PP polymer chains grafted onto the MWNTs sidewalls have indeed improved the interaction between TPO matrix and MWNTs significantly. Furthermore, covalently grafting polymer chains onto CNTs to improve their dispersion and interaction with polymers such as PMMA, polyethylene have already been shown to be effective in the literature.[18,35] The improvement in dispersion of MWNTs and their interaction with polymer matrix will be illustrated by SEM in the following part of this paper. In comparison, a 45% increase in modulus was obtained for TPO containing 5 wt % clay in the study carried out by Mishra et al.,[27] however a 35% decrease in elongation at break is obtained, indicating a decreased toughness. For TPO-based composites containing silica,[26] an improved toughness is obtained, but a decrease in modulus and strength is observed. Through the control on the adhesion between polymer matrix and filler, both strength and toughness of the prepared composites can be significantly improved by adding PP grafted

TABLE II
Mechanical Properties of Prepared Samples

Sample	Pure TPO	TPO/MWNTs	TPO/MWNTs-COOH	TPO/MWNTs-*g*-PP
Tensile strength (MPa)	6.2	4.1	4.5	8.0
Tensile modulus (MPa)	28	29	35	69
Elongation at break (%)	530	213	253	630
Toughness/(MJ/m^3)	25.7	7.1	9.4	43
Storage modulus (at 25°C) (MPa)	65	61	84	121

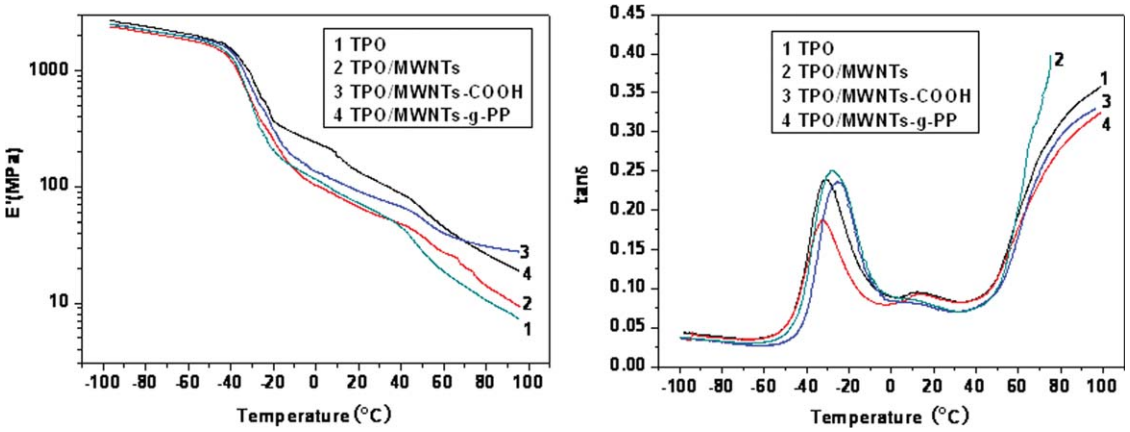

Figure 7 DMA curves of (a) Storage modulus as a function of temperature and (b) tan δ as a function of temperature for pure TPO (Curve 1), TPO/MWNTs (Curve 2), TPO/MWNTs-COOH (Curve 3), TPO/MWNTs-*g*-PP (Curve 4). [Color figure can be viewed in the online issue, which is available at wileyonlinelibrary.com.]

carbon nanotubes into TPO matrix in our study. It has been reported in the literature[42] that the increased attraction between nanofiller and rubbery polymer matrix would result in greater energy dissipation during tensile deformation, such an increase is caused by increased energy being dissipated during interfacial slippage.

Nevertheless, the tensile strength and elongation at break decreased when the raw MWNTs and MWNTs-COOH are added into TPO matrix (see Fig. 6). This indicates that the presence of weak interfacial bonding and poor dispersion of MWNTs.

Dynamic mechanical analysis

To confirm the mechanical reinforcing effect of MWNTs on TPO and study the effect of MWNTs on polymer chain mobility, dynamic mechanical analysis (DMA) was carried out. As shown in Figure 7(a), TPO/MWNTs-*g*-PP nanocomposites shows obvious enhancement in the storage modulus over the temperature range investigated. The enhancement of modulus is more significant in the rubbery region because of the soft and flexible nature of the material in this temperature region. As concluded from Table II, storage modulus of the TPO/MWNTs-*g*-PP is 90% higher than that of pure TPO at room temperature. The better enhancement in storage modulus for composites containing MWNTs-*g*-PP is due to better filler dispersion in the polymer matrix. While MWNTs-COOH shows moderate improvement in storage modulus, MWNTs-COOH is dispersed better in polymer matrix comparing with that of raw MWNTs.[29]

The variation of tan δ with the temperature of pure TPO and TPO/MWNTs nanocomposites is shown in Figure 7(b). For TPO/MWNTs-COOH and, the tan δ peak temperature (i.e., the glass transition temperature, T_g) of EPDM phase has shifted to a higher temperature, it is thought to be attributed by the reduced mobility of the polymer chains in the constrained environment. While a decrease in the T_g of TPO/MWNTs-*g*-PP is observed, which might be caused by the low molecular weight nature of PP chains in MWNTs-*g*-PP. Similar phenomena has been reported by Hwang et al.,[35] where a decrease in T_g has been obtained for poly(methyl methacrylate) (PMMA) based composites with the addition of PMMA-grafted MWNTs. Besides, a decrease of tan δ peak value for TPO/MWNTs-*g*-PP composites within the rubber transition temperature is attributed to a stronger filler-polymer interaction through surface absorption.[43]

Thermal stability of TPO/MWNTs nanocomposites

The thermal stability of TPO and MWNTs modified composites was characterized with TGA in nitrogen atmosphere. The TGA curves are shown in Figure 8. The initial thermal stabilities are characterized by

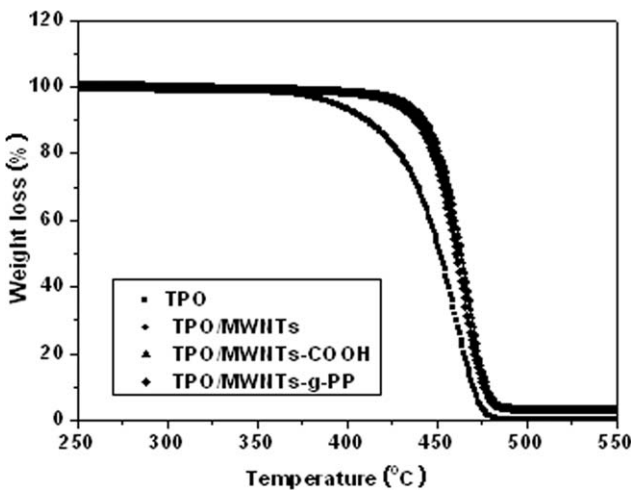

Figure 8 TGA analysis of TPO and TPO-based composites.

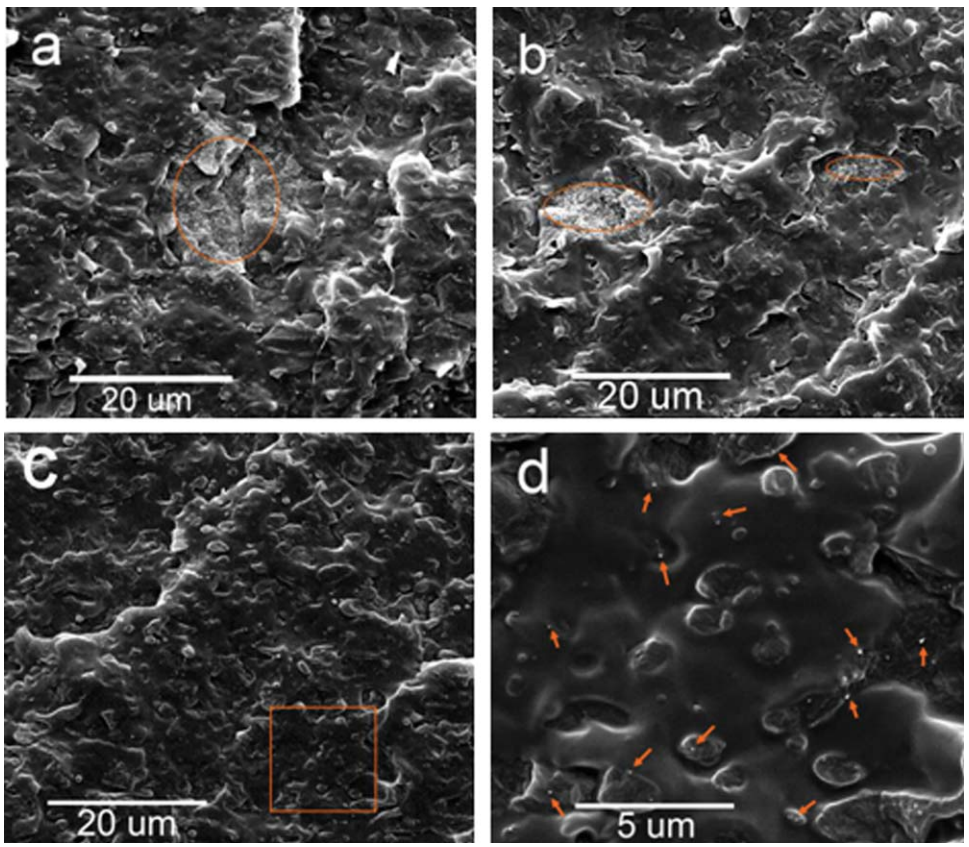

Figure 9 SEM micrographs of cold fractured surface of (a) TPO/MWNTs, (b) TPO/MWNTs-COOH, (c) TPO/MWNTs-*g*-PP. Please note that circus and arrows indicate the location of the MWNTs. [Color figure can be viewed in the online issue, which is available at wileyonlinelibrary.com.]

the temperatures at which 5% weight losses occurred, referred as $T_{-5\%}$. It can be observed that the degradation onset temperature of MWNTs modified composites is higher than that of neat TPO. The $T_{-5\%}$ of TPO-based composites is 30°C higher than neat TPO. The 50% loss temperature ($T_{-50\%}$) of TPO-based composites is also enhanced. While compare the system containing raw MWNTs, there is no obvious difference in thermal stability when modified MWNTs is added. The enhancement in the thermal stability of TPO is in a similar fashion as the ones reported for elastomer containing silica and clay.[44,45]

Morphology of TPO/MWNTs nanocomposites

To understand the effect of surface modification of MWNTs on the dispersion of MWNTs in TPO matrix and reveal the mechanism of mechanical reinforcement shown above, morphological study of the composites is carried out. As well known, homogeneous dispersion of MWNTs in polymer matrix is required for effective mechanical reinforcement of polymer matrix, as poor dispersion would lead to structural defects in composites. Here, cold fractured surface of TPO/MWNTs composites was characterized by SEM as shown in Figure 9. Many large aggregates can be found in the TPO/MWNTs composites containing raw MWNTs [see Fig. 9(a)]. This suggests that raw MWNTs have not been dispersed uniformly in the matrix because of the high interfacial energy between carbon nanotubes and nonpolar nature of TPO polymer matrix.[21]

In literature, Lee[20] reported that PP-*g*-MA has promoted a uniform dispersion of heat treated MWNTs in polypropylene matrix. It is thought that hydrogen bonds may be formed between the functional groups of PP-*g*-MA and modified MWNTs. In this work, it seems that PP-*g*-MA has minor effect on the dispersion of MWNTs-COOH as shown in Figure 9(b), as aggregates can still be found in the system. It might be caused by the strong van der Waals force among MWNTs-COOH, which makes the compacted MWNTs-COOH blocks hard to be dispersed by shear during melt blending. In fact, similar study in literature has reported that aggregates can still be found in the prepared composites containing MWNTs-COOH and polar polymers, such as polyamide.[40] The uniformly dispersed bright dots shows in Figure 9(c) suggest a good dispersion of MWNTs-*g*-PP throughout TPO matrix. The MWNTs-*g*-PP are embedded and tightly held to the matrix, which suggest a strong interfacial bonding between MWNTs-*g*-PP

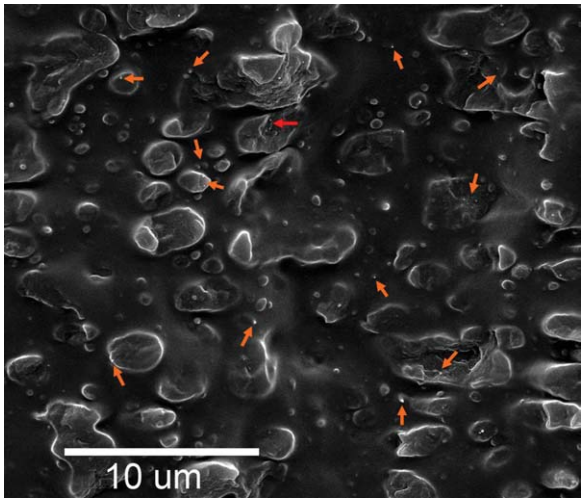

Figure 10 SEM micrographs of cold fractured and etched surface of TPO/MWNTs-*g*-PP. [Color figure can be viewed in the online issue, which is available at wileyonlinelibrary.com.]

and the TPO matrix. This would ensure better load transfer effect under tensile force. As a result, a significant improvement in mechanical properties is observed (see Fig. 6).

The distribution of fillers in polymer blends is considered to have great influence on the morphology, mechanical property, and electrical property of the composites.[26,46,47] According to Kontopoulou's study, stress transfer from matrix to dispersed phase is enhanced when filler is located in the continuous phase, meanwhile, the droplets are prohibited from coalescence during compounding.[25,26] The sample shown in Figure 8 is etched where EPDM phase is partially etched out to study the distribution of MWNTs-*g*-PP in TPO matrix. It can be noted that PP droplets as a dispersed phase located uniformly with small size. It is indicated by arrows in Figure 10 that MWNTs exist in both PP and EPDM phase with good dispersion. There are many factors control the distribution of filler in a binary blend, such as interfacial energy, viscosity of the blend components, preparation techniques.[28,48,49] In present work, the interfacial energy of PP is almost equal to that of EPDM,[28] so it is easy for MWNTs to migrate from PP phase to EPDM phase during processing. Therefore, MWNTs-g-PP is observed in both phases. Such a filler distribution status might be responsible for the mechanical reinforcement observed in this study, as both of phases are reinforced in this case.

CONCLUSION

Simultaneous strengthening and toughening is achieved through enhanced interfacial adhesion and improved filler dispersion in TPO matrix. To modify the interface between filler and matrix, two chemical modification methods, including treatment by acid, or covalently linkage with polypropylene, were applied on MWNTs to control the adhesion between nanofiller and TPO polymer matrix. FTIR and TGA results have shown that functional groups have been successfully grafted onto MWNTs. Morphological study has shown the effect of chemical modifications on the dispersion of MWNTs in TPO matrix, where the best dispersion is obtained for the composites containing MWNTs-*g*-PP. In agreement with morphological study, the prepared composites containing MWNTs-*g*-PP exhibited significant enhancement in strength, modulus, and toughness, indicating that the adhesion between MWNTs and TPO matrix has been improved dramatically. This study could be used as a guideline for strengthening and toughening TPO matrix in industrial applications.

References

1. Tasis, D. T. N.; Bianco, A.; Prato, M. Chem Rev 2006, 106, 1105.
2. Coleman, J. N.; Cadek, M.; Blake, R.; Nicolosi, V.; Ryan, K. P.; Belton, C.; Fonseca, A.; Nagy, J. B.; Gun'ko, Y. K.; Blau, W. J. Adv Funct Mater 2004, 14, 791.
3. Chen, Z. Y.; Kobashi, K.; Rauwald, U.; Booker, R.; Fan, H.; Hwang, W. F.; Tour, J. M. J Am Chem Soc 2006, 128, 10568.
4. Coleman, J. N.; Khan, U., Gun'ko, Y. K. Adv Mater 2006, 18, 689.
5. Coleman, J. N.; Khan, U.; Blau, W. J.; Gun'ko, Y. K. Carbon 2006, 44, 1624.
6. Wang, Z.; Ciselli, P.; Peijs, T. Nanotechnology 2007, 18, 455709.
7. Koshio, A.; Yudasaka, Y. M.; Zhang, M.; Iijima, S. Nano Lett 2001, 1, 361.
8. Li, S. Y.; Chen, H.; Bi, W. G.; Zhou, J. J.; Wang, Y. H.; Li, J. Z.; Cheng, W. X.; Li, M. Y.; Li, L.; Tang, T. J Polym Sci Part: Polym Chem 2007, 45, 5459.
9. Tang, W. Z.; Santare, M. H.; Advani, S. G. Carbon 2003, 41, 2779.
10. Zhu, J.; Peng, H. Q.; Rodriguez-Macias, F.; Margrave, J. L.; Khabashesku, V. N.; Imam, A. M.; Lozano, K.; Barrera, E. V. Adv Funct Mater 2004, 14, 643.
11. Peng, H. Q.; Alemany, L. B.; Margrave, J. L.; Khabashesku, V. N. J Am Chem Soc 2003, 125, 15174.
12. Moniruzzaman, M.; Winey, K. I. Macromolecules 2006, 39, 5194.
13. Bose, S.; Khare, R. A.; Moldenaers, P. Polymer 2010, 51, 975.
14. Yang, J. H.; Wang, C. Y.; Wang, K.; Zhang, Q.; Chen, F.; Du, R. N.; Fu, Q. Macromolecules 2009, 42, 7016.
15. Hou, Z. C.; Wang, K.; Zhao, P.; Zhang, Q.; Yang, C. Y.; Chen, D. Q.; Du, R. N.; Fu, Q. Polymer 2008, 49, 3582.
16. Liu, T. X.; Phang, I. Y.; Shen, L.; Chow, S. Y.; Zhang, W. D. Macromolecules 2004, 37, 7214.
17. Shen, J. D.; Huang, W. S.; Wu, L. P.; Hu, Y. Z.; Ye, M. X. Mater Sci Eng A 2007, 464, 151.
18. Yang, B. X.; Pramoda, K. P.; Xu, G. Q.; Goh, S. H. Adv Funct Mater 2062 2007, 17.
19. Yang, B. X.; Shi, J. H.; Pramoda, K. P.; Goh, S. H. Compos Sci Technol 2008, 68, 2490.
20. Lee, S. H.; Cho, E.; Jeon, S. H.; Youn, J. R. Carbon 2007, 45, 2810.
21. Pan, Y. Z.; Li, L.; Chan, S. H.; Zhao, J. H. Composites Part A 2010, 41, 419.

22. Zhang, Z. N.; Zhang, J.; Chen, P.; Zhang, B. Q.; He, J. S.; Hu, G. H. Carbon 2006, 44, 692.
23. Liu, Y. T.; Zhao, W.; Huang, Z. Y.; Gao, Y. F.; Xie, X. M.; Wang, X. H.; Ye, X. Y. Carbon 2006, 44, 1613.
24. Lee, H. S.; Fasulo, P. D.; Rodgers, W. R.; Paul, D. R. Polymer 2005, 46, 11673.
25. Kontopoulou, M.; Liu, Y. Q.; Austin, J. R.; Parent, J. S. Polymer 2007, 48, 4520.
26. Liu, Y. Q.; Kontopoulou, M. Polymer 2006, 47, 7731.
27. Mishra, J. K.; Hwang, K. J.; Ha, C. S. Polymer 1995 2005, 46.
28. Yang, H.; Zhang, Q.; Guo, M.; Wang, C.; Du, R. N.; Fu, Q. Polymer 2006, 47, 2106.
29. Valentini, L.; Biagiotti, J.; Kenny, J. M.; Manchado, M. A. L. J Appl Polym Sci 2003, 89, 2657.
30. Hom, S.; Bhattacharyya, A. R.; Khare, R. A.; Kulkarni, A. R.; Saroop, M.; Biswas, A. Polym Eng Sci 2009, 49, 1502.
31. Ramanathan, T.; Fisher, F. T.; Ruoff, R. S.; Brinson, L. C. Chem Mater 2005, 17, 1290.
32. Tang, C. Y.; Xiang, L. X.; Su, J. X.; Wang, K.; Yang, C. Y.; Zhang, Q.; Fu, Q. J Phys Chem B 2008, 112, 3876.
33. Shao, W. G.; Wang, Q.; Wang, F.; Chen, Y. H. Carbon 2006, 44, 2708.
34. Li, W. H.; Chen, X. H.; Yang, Z.; Xu, L. S. J Appl Polym Sci 2009, 113, 3809.
35. Hwang, G. L.; Shieh, Y. T.; Hwang, K. C. Adv Funct Mater 2004, 14, 487.
36. Dettlaff-Weglikowska, U.; Benoit, J. M.; Chiu, P. W.; Graupner, R.; Lebedkin, S.; Roth, S. Curr Appl Phys 2002, 2, 497.
37. Zhang, Y. C.; Broekhuis, A. A.; Stuart, M. C. A.; Landaluce, T. F.; Fausti, D.; Rudolf, P.; Picchioni, F. Macromolecules 2008, 41, 6141.
38. Shi, J. H.; Yang, B. X.; Goh, S. H. Eur Polym Mater 2009, 45, 1002.
39. Li, J.; Fang, Z. P.; Tong, L. F.; Gu, A. J.; Uu, F. J Appl Polym Sci 2007, 106, 2898.
40. Meng, H.; Sui, G. X.; Fang, P. F.; Yang, R. Polymer 2008, 49, 610.
41. Wang, Y. B.; Iqbal, Z.; Malhotra, S. V. Chem Phys Lett 2005, 402, 96.
42. Wang, T.; Lei, C. H.; Liu, D.; Manea, M.; Asua, J. M.; Creton, C.; Dalton, A. B.; Keddie, J. L. Adv Mater 2008, 20, 90.
43. Bazgir, S.; Katbab, A. A.; Nazockdast, H. J Appl Polym Sci 2004, 92, 2000.
44. Austin, J. R.; Kontopoulou, M. Polym Eng Sci 2006, 46, 1491.
45. Wu, T. M.; Chu, M. S. J Appl Polym Sci 2005, 98, 2058.
46. Goldel, A.; Kasaliwal, G.; Potschke, P. Macromol Rapid Commun 2009, 30, 423.
47. Zou, H.; Wang, K.; Zhang, Q.; Fu, Q. Polymer 2006, 47, 7821.
48. Elias, L.; Fenouillot, F.; Majeste, J. C.; Cassagnau, P. Polymer 2007, 48, 6029.
49. Fenouillot, F.; Cassagnau, P.; Majeste, J. C. Polymer 2009, 50, 1333.